Hybrid Control of Force Transients for Multi-point Injection Engines.

A. Balluchi[†] L. Benvenuti[†§]
M. D. Di Benedetto[‡] A. L. Sangiovanni–Vincentelli[†¶]
[†]PARADES, Via San Pantaleo, 66, 00186 Roma, Italy,
balluchi, lucab, alberto@parades.rm.cnr.it
[§]Dip. di Informatica e Sistemistica, Università degli Studi di Roma "La Sapienza",
Via Eudossiana 18, 00184 Roma, Italy, benve@dis.uniroma1.it
[‡]Dip. di Ingegneria Elettrica, Università degli Studi de L'Aquila,
Poggio di Roio, 67040 L'Aquila, Italy, dibenede@ing.univaq.it
[¶]Dep. of Electrical Engineering and Computer Science,
University of California at Berkeley, CA 94720, alberto@eecs.berkeley.edu

Abstract

We address the problem of delivering as quickly as possible a requested torque produced by a spark ignition engine equipped with a multi-point port injection manifold and with electronic throttle. The optimal control problem, subject to the constraint that the air–fuel ratio stays within a pre–assigned range around the stoichiometric ratio, is solved for a detailed, cycle-accurate hybrid model with a hybrid control approach based on a two-step process. In the first step, a continuous approximation of the hybrid problem is solved exactly. Then, the control law so obtained is adjusted to satisfy the constraints imposed by the hybrid model. The quality of the control law has been in part analytically demonstrated and in part validated with simulations.

1 Introduction

In this paper, we deal with the problem of delivering as quickly as possible a requested torque produced by a spark ignition engine equipped with a multi-point port injection manifold and electronics to control the throttle-valve position. The control variables are: the amount of injected fuel and the voltage given to the electric motor controlling the position of the throttle valve. The optimization problem is subject to the constraint that the air–fuel (A/F) ratio stays within a pre–assigned range around the stoichiometric value of 14.64 (the ratio that guarantees minimum emission). Air and fuel dynamics depend on the pressure in the intake manifold - that is controlled by throttle valve - and on second order phenomena, the most important of which is the fluid film dynamics [8]. The fluid film is created during the injection process: after fuel is injected in the intake runner, part of the vaporized fuel turns into fluid that deposits onto the walls of the intake runner and, hence, it is not immediately available for combustion inside the cylinders. The fluid film on the intake walls evaporates again, thus contributing to the combustion process but with a noticeable delay. This phenomenon (unfortunately) cannot be ignored, since it has a definite effect on the performance of the combustion process.

The most used solutions to this problem consist of feed-forward compensation of fuel dynamics [1, 9, 6], based on mean value engine models [5, 10, 7]. However, the mean values of the engine variables of interest may not be accurate enough to guarantee small transient deviations from the optimal A/F ratio. In this paper, we propose an approach that yields very small deviations with respect to the optimal A/F ratio, by using a hybrid model of the cyclic behavior of the engine. The hybrid model describes accurately the detailed behavior of the actuated throttle, of the injection systems and of the torque-generation mechanism, and, at the same time, allows to develop powerful closed-loop control laws.

Our goal is to design a control law for the fuel injection durations and the voltage supplied to the throttle valve motor to drive the evolution of the system from an initial condition characterized by the delivery of a torque u^0 to a final condition characterized by the delivery of a requested torque u^1 in minimum time subject to constraints on emissions. Note that the control problem described above is new not only because we use a detailed hybrid model for the injection process but also because we consider the entire control chain, from throttle motor to engine.

Minimum-time is not the only relevant criterion to follow when considering control schemes that might be implemented for engine control. Preventing significant over/undershoot of the reference value, and being able to hold the desired torque value within some bounds are also desirable. However, minimum-time control problems have well-known solutions that allow us to obtain powerful control laws. These additional criteria can be cast into constraints in the same way as we have done for the A/F ratio. Then, the optimal control problem can still be solved analytically even though the number of details and the notational complexity would become overwhelming. For this reason, we have chosen to ignore these additional considerations since handling them could cloud our approach.

Our approach to the optimal control problem is a two-step process:

1. we first introduce and solve an auxiliary optimal control problem in continuous time, and

2. we then map the optimal control law back in the hybrid domain trying to maintain as much as possible the properties of the solution.

The mapping process is critical for obtaining a satisfactory solution to the hybrid problem. Several mappings are possible that satisfy the restrictions imposed by the hybrid model but we want to choose a mapping that satisfies the original constraints and is as close as possible to the optimal solution. In [2], we have solved with the same approach a related, but simpler, problem where throttle actuation was not taken into account, the torque requested was zero and the cost function was the amount of undesired oscillations of the power–train (the cut-off problem). In this case, we were able to prove that the hybrid control law obtained by the mapping process ensured stability and constraints satisfaction. In this paper, given the additional details that have been considered, the control law obtained by the two-step process is more complex and depends on several engine and car parameters. For this reason, the theoretical results are weaker, but, under conservative assumptions on the relative speed of the crankshaft at the time of successive injection points and ignoring the dynamics of the throttle control loop, we can still prove that the original constraints on the problem are satisfied with the hybrid control law. Simulation data are used to validate the control laws for the full chain on power–trains of existing cars.

It can be argued that a dual approach, relying on a discretized, crank-angle based abstraction of the cylinder's FSM (see for example [4]), would solve the problem tackled in this paper as well. Since we assume small excursions in engine speed, then the phase of mapping the auxiliary optimal solution into the hybrid domain is likely to be easier when discrete–time abstractions are used with respect to continuous–time ones. Indeed, the cut–off problem has also been solved using this approach [3], i.e., a discrete–time abstraction of the hybrid model of the plant was used. However, the weakness of this approach lays on the lack of theoretical results asserting properties of the control law since only numerical solutions to the auxiliary optimal discrete–time control problem can be obtained.

2 Plant model and problem formulation

In this section, a hybrid model for vehicles with 4–stroke 4–cylinder gasoline engine equipped with a multi–point injection system and electronic throttle is illustrated. The model (an expansion of the model in [2]) consists of four parts (see Fig. 1): two continuous-time systems, modeling the power-train dynamics and the air dynamics respectively, and two parts each composed of four hybrid systems modeling the behavior of each cylinder and of each injection system.

Air Dynamics. The model of the quantity of air entering the cylinder during the intake run is obtained from the air flow balance equation of the manifold. The air mass m_a, loaded during an intake run, is subject to the manifold pressure (p) dynamics which is controlled by the throttle valve actuated by a DC motor. Since we consider short control horizon, then we can assume small variations of the crankshaft speed and neglect the dependence from it in the air dynamics. The model is then

$$\dot{\alpha}(t) = a_\alpha\, \alpha(t) + b_\alpha v(t) \tag{1}$$

$$\dot{p}(t) = a_p\, p(t) + b_p \alpha(t) \tag{2}$$

$$m_a(t) = c_p\, p(t) \tag{3}$$

where $v \in [-V, +V]$ is the DC motor voltage and α is the throttle angle that is subject to the constraint

$$0 \leq \quad \alpha(t) \quad \leq 90\,. \tag{4}$$

Powertrain Model. Powertrain dynamics are modeled by the linear system

$$\dot{\zeta}(t) = A\,\zeta(t) + b\,u(t),$$

where $\zeta = [\alpha_e, \omega, \omega_p]^T$ represents the axle torsion angle, the crankshaft revolution speed and the wheel revolution speed. The input signal u is the torque produced by the engine and acting on the crankshaft. Model parameters A and b, depend on the transmission gear which is assumed not to change. A single-state hybrid system emits the event *dead_point*, when pistons reach either the top or bottom dead centers, and produces the crank angle ϕ.

Torque-generation. The behavior of each cylinder in the engine is abstractly represented by a Finite State Machine (FSM) and a Discrete Event System (DES) modeling torque generation. The FSM state S_i of the i–th cylinder assumes values in the set $\{H_i, I_i, C_i, E_i\}$ which correspond to the Exhaust, Intake, Compression and Expansion strokes, respectively, in the 4-stroke engine cycle. A FSM transition occurs when the piston reaches a dead center, that is when the event *dead_point* is emitted. The DES describing the torque generation process of the i–th cylinder increments its sequence index k by one at each transition of the FSM. Its inputs are the masses m_{ai} and m_{vi} of air and fuel loaded during the intake phase; its output is the torque $u_i(k)$ generated by the cylinder. At the transition $I_i \to C_i$, that is at time t_{Ii}, the event int_end_i is generated and the DES reads its inputs, storing in q_{ai} and q_{vi} their values. The amount of torque achievable during the next expansion phase, obtained by the fuel-to-torque gain G, is stored in z_i. The DES output $u_i(k)$ is always zero except at the $C_i \to E_i$ transition when it is set to the value stored in z_i. Input $u_i(t)$ to the powertrain dynamics is obtained from $u_i(k)$ by a zero–order holder latched on the event *dead_point*.

Injection Process. The i-th injection system is abstractly represented by a hybrid system, whose discrete state F_i assumes values in the set $\{J_i, B_i, W_i, D_i\}$ described below:
• J_i: the injector is open and delivers a constant flow P of vaporized fuel. A fraction χ of it condenses in a fuel-puddle and increases the mass m_{li} of liquid fuel, fraction $1-\chi$ increases the mass m_{vi} of vaporized fuel in the intake runner. The mass of liquid fuel evaporates off with a time constant τ. The injector remains open for Δ_i seconds modeled by timer t_i''.
• B_i: the injector is closed and the evaporation process continues. When the next *dead_point* event is emitted, the intake valve opens, and the air-fuel mix begins to enter the cylinder. At the $I_i \to C_i$ transition, the intake valve closes and the int_end_i event is generated. The mass m_{vi} of vapor is reset to zero since all the vapor fuel has been loaded in the cylinder.
• W_i: the injector is closed and evaporation proceeds.
• D_i: the beginning of fuel injection is synchronized with respect to the beginning of the exhaust phase with a time delay of t_d seconds measured by timer t_i'. This delay allows to locate the injection interval with respect to the engine cycle. The value of t_d, which in general depends on the crankshaft speed, is considered constant since small engine speed variations are assumed. In this state, fuel dynamics is as in state W_i.

Engine hybrid model. The overall model $\mathcal{E}$ of the engine is the combination of four hybrid systems representing the behavior of each cylinder and related injection system, and the power-train and intake manifold models which are shared among all cylinders. The pistons are connected to the crankshaft, so that dead-points are synchronous and the cycle of each one is delayed one step with respect to the cycle of the previous one. Then, the *dead_point* events and the sequence index k are shared among all the cylinders and only one signal $u_i(t)$ may be different from zero at any time. Input signals are: the input voltage $v(t)$ to the DC motor actuating the throttle valve, a scalar continuous time signal in the class of functions $\mathbb{R}_0^+ \to [-V, +V]$; the injection intervals $\Delta(k)$, a scalar discrete time signal in the class of functions $\mathbb{Z}_0^+ \to [0, \Delta_{max}]$, which is sequentially distributed over the four injectors synchronously with the corresponding exp_end_i event.

The state of the overall hybrid systems is a triple $(\mathbf{q}, \mathbf{z}, \mathbf{x})$ where:

- $\mathbf{q} = [S_1, F_1, S_2, F_2, S_3, F_3, S_4, F_4]$ is the state of the FSMs associated to each cylinder and each injection system;
- $\mathbf{z} = [z_1, q_{v1}, q_{a1}, \ldots, z_4, q_{v4}, q_{a4}]$ is the cylinder DES state;

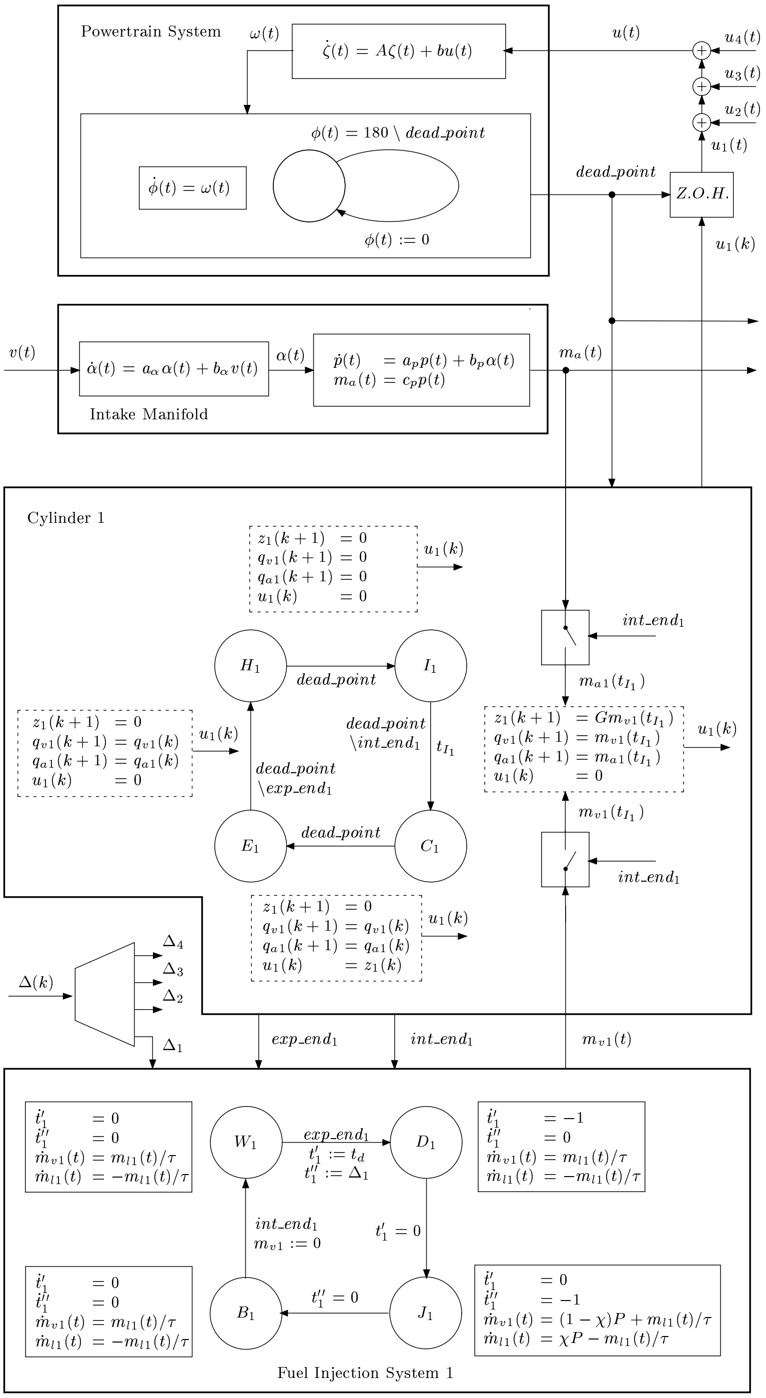

Figure 1: Engine hybrid model $\mathcal{E}$. The hybrid models of the cylinders and injection systems 2, 3 and 4 are not reported due to space limitation.

- $\mathbf{x} = [\zeta, \phi, \alpha, p, t_1', t_1'', m_{v1}, m_{l1}, \ldots, t_4', t_4'', m_{v4}, m_{l4}]$ is the continuous state associated to the powertrain, air dynamics, and to each injection system.

The output of the overall system is the generated torque u.

2.1 Problem formulation

In order to reduce tailpipe emissions, the air-fuel ratio A/F of each cylinder has to be kept in a range $[L_{min}, L_{max}]$ around the stoichiometric value $L_{stc} = 14.64$. This corresponds to requiring the following constraint:

$$L_{min}\, q_{vi_C}(k) \leq \; q_{ai_C}(k) \; \leq L_{max}\, q_{vi_C}(k)\,, \tag{5}$$

where i_C denotes the index of the cylinder which enters the state C.

Given a value $\tilde{u}$ of torque produced by the engine, define in the hybrid state space the set $\mathcal{T}(\tilde{u})$ of all the hybrid states $(\mathbf{q}(0), \mathbf{z}(0), \mathbf{x}(0))$ for which there exist $\tilde{v}(t) : \mathbb{R}_0^+ \to [-V, +V]$ and $\tilde{\Delta}(k) : \mathrm{Z}_0^+ \to [0, \Delta_{max}]$ such that for all $t \geq 0$ and for all $k \geq 0$, $u(t) = \tilde{u}$ and constraints (4) and (5) are satisfied.

Note that the set $\mathcal{T}(\tilde{u})$ consists of all the state trajectories of the hybrid model $\mathcal{E}$ such that along the entire trajectories a constant torque $\tilde{u}$ is generated while constraints on inputs v, Δ and states α, q_a, q_v are satisfied.

Problem 1 *Consider the engine hybrid model $\mathcal{E}$, shown in Figure 1. Let u^0 and u^1 be the initial value and the desired value of the torque, respectively. Assume that, at the initial time $t = 0$, the hybrid state $(\mathbf{q}^0, \mathbf{z}^0, \mathbf{x}^0)$ belongs to $\mathcal{T}(u^0)$. Find $\hat{v}(t) : \mathbb{R}_0^+ \to [-V, +V]$ and $\hat{\Delta}(k) : Z_0^+ \to [0, \Delta_{max}]$ such that*

- *the initial state $(\mathbf{q}^0, \mathbf{z}^0, \mathbf{x}^0)$ is steered to $\mathcal{T}(u^1)$ at some unspecified time $t^\star$;*
- *for all $t \geq 0$ and for all $k \geq 0$ constraints (4) and (5) are satisfied;*
- *the time $t^\star$ is minimized.*

3 Auxiliary continuous–time optimal control without throttle dynamics

In this section, the interactions between fuel and air dynamics, subject to constraint (5), are analyzed by considering a continuous–time model approximating the behavior of the engine hybrid model $\mathcal{E}$. The hybrid nature of the intake process is abstracted away by using average continuous–time models for fuel and air whose outputs are the average fuel flow, $f_v(t)$, and air flow, $f_a(t)$, entering the cylinders. Moreover, we abstract away the throttle actuation dynamics and consider the throttle valve to be the air dynamics input.

To solve the continuous optimal problem, we follow a two-step process: in the first step, we find the minimum–time control for the air dynamics alone; in the second step, we introduce the fuel dynamics and appropriately modify the optimal control law found in the first step to solve the continuous optimal problem at hand.

The intake manifold dynamics is described by equation (2) and constraint (4). The flow of air $f_a(t)$ entering the cylinders is expressed as:

$$f_a(t) = c_a p(t) \,,$$

where $c_a = \frac{\omega^0}{30} c_p$. Furthermore, fuel dynamics is modeled by the average model

$$\begin{aligned} \dot{\overline{m}}_l(t) &= a_l \overline{m}_l(t) + b_l \Delta(t) \\ f_v(t) &= c_l \overline{m}_l(t) + d_l \Delta(t) \end{aligned} \tag{6}$$

where f_v denotes the average fuel flow entering the cylinders, $\overline{m}_l$ denotes the average mass of liquid fuel, and $a_l = -\tau^{-1}$, $b_l = \chi P \frac{\omega^0}{30}$, $c_l = \tau^{-1}$, $d_l = (1-\chi) P \frac{\omega^0}{30}$.

The A/F constraints are rewritten for the flows f_a and f_v as follows

$$L_2 p(t) + L_m \overline{m}_l(t) \le \Delta(t) \le L_1 p(t) + L_m \overline{m}_l(t) \,, \tag{7}$$

where $L_1 = \frac{c_a}{L_{min} d_l} > 0$, $L_2 = \frac{c_a}{L_{max} d_l} > 0$, and $L_m = -\frac{c_l}{d_l} < 0$. For the continuous time model here considered, the target set corresponding to the desired torque u^1 is

$$\overline{\mathcal{T}}(u^1) = \left\{ (\overline{m}_l, p) |\; p = p^1 = \frac{14.64}{c_p G} u^1 \right\} , \tag{8}$$

so that Problem 1 reduces to the following one:

Problem 2 *Consider the engine continuous–time model described by equations (2) and (6). Let u^0 and u^1 be the initial value and the desired value of the torque, respectively. Assume that, at the initial time $t = 0$, the state $(\overline{m}_l^0, p^0)$ belongs to $\overline{\mathcal{T}}(u^0)$. Find $\hat{\alpha}(t) : \mathbb{R}_0^+ \to [0, 90]$ and $\hat{\Delta}(t) : \mathbb{R}_0^+ \to [0, \Delta_{max}]$ such that*

- *the initial state $(\overline{m}_l^0, p^0)$ is steered to $\overline{\mathcal{T}}(u^1)$ at some unspecified time $t^\star$;*
- *for all $t \ge 0$, constraints (7) are verified;*
- *the time $t^\star$ is minimized.*

Constraints (7) define a set of feasible values for $(\overline{m}_l, p)$, obtained for Δ ranging in the interval $[0, \Delta_{max}]$. Since the liquid fuel mass is nonnegative, the set of feasible states for the control problem at hand are defined by the following linear inequalities

$$\begin{array}{l} L_1 p + L_m \overline{m}_l \ge 0 \\ L_2 p + L_m \overline{m}_l \le \Delta_{max} \\ p, \overline{m}_l \ge 0 \end{array} \tag{9}$$

Note that, when the manifold pressure p is zero, the unique feasible state value is $(\overline{m}_l, p) = (0, 0)$, which is obtained with injection $\Delta = 0$ (neither fuel nor air is loaded by the cylinders). As a matter of fact, the evaporation of any liquid fuel $\overline{m}_l > 0$ would produce a rich mixture with $\frac{f_a}{f_v} < L_{min}$. Hence, if a fuel puddle is present, the manifold pressure has to be greater than zero. However, by injecting a proper amount of fuel, some values $(\overline{m}_l, p)$ on the line $\overline{m}_l = 0$ may be feasible even if there is no fuel puddle. These values lay on the segment

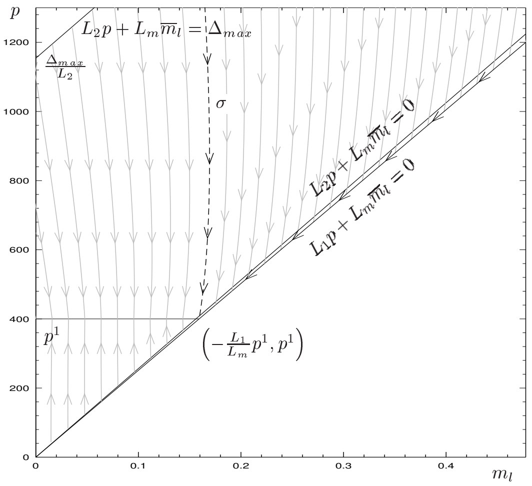

Figure 2: Minimum–time trajectories without throttle dynamics.

with extremum points $(0, 0)$ and $(0, \Delta_{max}/L_2)$. Note that only the segment from $(0, p^1)$ to $(-(L_1/L_m)p^1, p^1)$ of the target set $\overline{\mathcal{T}}(u^1)$ belongs to the feasible set (9). Constraints (7) couples between the manifold dynamics (2) and the fuel dynamics (6). If one considers the manifold dynamics (2) alone, the straightforward minimum–time control to the target point $p = p^1$ is:

$$\alpha = \begin{cases} 0 & \text{if } p > p^1 \\ 90 & \text{if } p < p^1 \\ -(a_p/b_p)p^1 & \text{when } p = p^1 \end{cases} . \tag{10}$$

The minimum–time $t^\star$ needed to steer an initial manifold pressure $p(0)$ to p^1 is

$$t^\star = \begin{cases} \frac{1}{a_p} \ln(\frac{p^1}{p(0)}) & \text{if } p(0) > p^1 \\ \frac{1}{a_p} \ln(\frac{a_p p^1 + 90\, b_p}{a_p p(0) + 90\, b_p}) & \text{if } p(0) < p^1 \end{cases} . \tag{11}$$

Given an initial fuel value $\overline{m}_l(0)$, the manifold control (10) remains optimal when the fuel dynamics (6) are also considered and the constraints (7) are introduced, if there exists a fuel injection signal $\Delta(t) : [0, t^\star] \to [0, \Delta_{max}]$ such that constraints (7) are satisfied along the trajectory. In fact, if this is the case, the trajectory $(\overline{m}_l(t), p(t))$ starting from $(\overline{m}_l(0), p(0))$ reaches the target set $\overline{\mathcal{T}}(u^1)$ at time $t^\star$ without leaving the feasible set defined by (9).

In the following we will:

- find the feasible initial conditions for which the control law (10) remains optimal;
- give the optimal control law for the remaining initial conditions.

Consider first the initial conditions $(\overline{m}_l(0), p(0))$ in the region delimited by (9) and $p < p^1$, where the control $\alpha = 90$ is applied. For these conditions it can be shown that there are always values of Δ satisfying (7) along the entire trajectory to the target set. Then, the control law

$\alpha = 90$ and Δ equal to any value satisfying (7) steer the state to the target set in minimum time satisfying the constraints. In this case, the time required to drive the initial condition to the target set is determined only by the pressure dynamics and is given by (11).

On the other hand, when $p(0) > p^1$ and the control $\alpha = 0$ is applied, it can be the case that no value of Δ satisfying (7) exists for some point of the trajectory. Since $p(t)$ is decreasing, this corresponds to violating the constraint $\frac{f_a}{f_v} > L_{min}$. To avoid (if possible) this situation, the amount of fuel flow entering the cylinders has to be minimized, by choosing the minimum admissible value for Δ, i.e., $\Delta = \max\{0, L_2 p + L_m \overline{m}_l\}$. Then, for the initial conditions $(\overline{m}_l(0), p(0))$ in the region delimited by (9) and $p > p^1$, where the control $\alpha = 0$ is applied, there are always values of Δ satisfying (7) along the entire trajectory to the target set provided that $(\overline{m}_l(0), p(0))$ is on the left of the trajectory σ obtained by backwards integration of dynamics (2) and (6) from the point $(-(L_1/L_m)p^1, p^1)$ with $\alpha = 0$ and $\Delta = \max\{0, L_2 p + L_m \overline{m}_l\}$. (See Figure 2). Hence, for these initial conditions, applying the control law $\alpha = 0$ and Δ equal to any value satisfying (7), the target set is reached in minimum time and the constraints are satisfied. Also in this case, the time needed to steer the initial condition to the target set is determined only by the pressure dynamics and is given by equation (11).

In summary, for all the initial conditions in the feasible set (9) and on the left of σ, the optimal controls are

$$\alpha = \begin{cases} 0, & \text{if } p > p^1 \\ 90, & \text{if } p < p^1 \end{cases} \qquad \text{and} \qquad \Delta = \max\{0, L_2 p + L_m \overline{m}_l\}\,.$$

Fuel dynamics is steered in such a way that it tracks the intake manifold dynamics to satisfy the air–fuel constraint (7). Since the amount of fuel puddle is small with respect to the values of the manifold pressure, then the air dynamics can be controlled in minimum time to the target pressure p^1, without any interference due to the air–fuel constraint, which is handled by the injection signal only.

For conditions $(\overline{m}_l(0), p(0))$ in the region delimited by (9) and lying to the right of the curve σ, the air dynamics has to track the slower fuel evaporation dynamics to achieve air–fuel constraint (7) satisfation. Hence, for these initial conditions, the optimal feedback controls are as follows:

$$\alpha = \begin{cases} 0, & \text{if } L_1 p + L_m \overline{m}_l > 0 \\ \frac{a_l - a_p}{b_p} p, & \text{if } L_1 p + L_m \overline{m}_l = 0 \end{cases} \qquad \text{and} \qquad \Delta = \max\{0, L_2 p + L_m \overline{m}_l\}\,. \tag{12}$$

According to (12), these initial conditions are first steered by the controls $\alpha = 0$ and $\Delta = \max\{0, L_2 p + L_m \overline{m}_l\}$ to the line $L_1 p + L_m \overline{m}_l = 0$. Then, under the action of the control signals $\alpha = \frac{a_l - a_p}{b_p} p$ and $\Delta = 0$, they follow a sliding motion along this constraint until they reach the extremum $(-(L_1/L_m)p^1), p^1)$ of the target set. It is worth noting that during the sliding motion, the closed–loop system is

$$\begin{array}{l} \dot{\overline{m}}_l(t) = a_l \overline{m}_l(t) \\ \dot{p}(t) = a_p p + b_p \frac{a_l - a_p}{b_p} p = a_l p \end{array}\,.$$

Since $|a_l| < |a_p|$, the pressure dynamics is slowed down to make it follow the fuel dynamics and to satisfy constraints (7). Thus, the control law for Δ given by (12) is optimal since it minimizes the length of the arc of trajectory over the constraint. Summarizing:

Theorem 1 *If the initial state $(\overline{m}_l^0, p^0)$ belongs to the feasible set described by inequalities (9), then the optimal control $\hat{\alpha}(t) : \mathbb{R}_0^+ \to [0, 90]$ and $\hat{\Delta}(t) : \mathbb{R}_0^+ \to [0, \Delta_{max}]$ solving Problem 2 is:*

$$\hat{\alpha}(t) = \begin{cases} 0 & \text{if } L_1 p(t) + L_m \overline{m}_l(t) > 0 \text{ and } p(t) > p^1, \\ 90 & \text{if } p(t) < p^1, \\ -(a_p/b_p)p^1 & \text{if } p(t) = p^1, \\ \frac{a_l - a_p}{b_p} p(t) & \text{if } L_1 p(t) + L_m \overline{m}_l(t) = 0 \text{ and } p(t) > p^1 \end{cases} \tag{13}$$

$$\hat{\Delta}(t) = \max\{0, L_2 p(t) + L_m \overline{m}_l(t)\}. \tag{14}$$

This result can be proved by applying the Pontryagin Maximum Principle. Figure 2 shows some minimum–time trajectories to the target set (8) for dynamics (2) and (6), and constraints (7).

4 Hybrid control without throttle dynamics

The continuous control law described in Section 3, must be approximated to yield a feasible control law for the hybrid model $\mathcal{E}$ introduced in Section 2. More precisely, in the continuous time model adopted in Section 3, the air–fuel constraints (7) are expressed in terms of the continuous evolutions of the manifold pressure and liquid fuel. Moreover, the control signals α and Δ are assumed to be continuous–time signals. When dealing with the hybrid model $\mathcal{E}$, the air–fuel constraints (5) are expressed in terms of the event–based signals q_a and q_v. In addition, the amount of air q_a loaded in the cylinder depends on the manifold pressure p at the dead center corresponding to the end of the intake. The amount of loaded fuel q_v depends on the evolution of the hybrid model describing the fuel injection system, which models the delay between the time at which the injection control signal Δ is set and the time at which the fuel is loaded.

Then, the main issues to address when we move from the continuous case to the hybrid case are:

- in model $\mathcal{E}$ there is a delay between the time at which the injection control Δ_i is set (at the end of the expansion phase) and the time at which the vaporized fuel q_v is loaded (at the end of the intake phase);
- feasible control actions on Δ_i are discrete-time signals synchronized with the crank angle. This issue is the main cause of difficulty for devising a hybrid control strategy;
- in model $\mathcal{E}$, there exist four independent fuel dynamics, controlled by inputs $\Delta_1, \ldots, \Delta_4$, whose evolutions are constrained with respect to the same air flow evolution by A/F bounds.

The measurements available for closing the control loop are: the pressure p, the angle α and the crankshaft speed ω. Since in the solutions derived in Section 3, Δ is chosen as the maximum between 0 and $L_2 p + L_m \overline{m}_l$, then fuel injection is regulated so to maintain in (5) $q_a = L_{max} q_v$, when the cylinder is in the compression stroke. The injection control Δ_i for the i-th cylinder is set at the end of the expansion stroke (i.e., when the *exp_end*$_i$ event is generated).

Consider first the design of the fuel injection control. The continuous optimal injection control law (14) has only two possible actions: either no fuel is injected, that is $\Delta = 0$; or $\Delta = L_2 p + L_m \overline{m}_l$, which corresponds to producing a mixture with maximum feasible value of A/F ratio, is injected.

Hence, our strategy is mapped into the hybrid domain as follows. At time t_k, corresponding to the end of the expansion stroke, the value of Δ is set to one of the two possible values on the basis of the estimated values of $q_a(k+2)$ and $q_v(k+2)$ at time t_{k+2} corresponding to the end of the next intake stroke:

($\mathbf{\Delta}$1) either $\Delta(k) = 0$, i.e. if $q_a(k+2) < L_{max} q_v(k+2)$ no fuel is injected;

($\mathbf{\Delta}$2) or $\Delta(k)$ such that $q_a(k+2) = L_{max} q_v(k+2)$, i.e. a mixture with maximum feasible value of A/F ratio is produced (see (5)).

The estimations of $q_a(k+2)$ and $q_v(k+2)$ are non trivial since they depend not only on the values of the state components $\omega(t_k)$, $m_v(k)$, $m_l(k)$ and $p(t_k)$, but also on the chosen control actions $\Delta(k)$ and $\alpha(t)$ over $[t_k, t_{k+2}]$.

Consider now the design of the throttle control. The continuous minimum–time control (13) assumes only four possible values: $\alpha = 0$, $\alpha = 90$, $\alpha = (a_l - a_p/b_p)p$ and finally $\alpha = -(a_p/b_p)p^1$ when the target set has been reached.

This strategy is mapped into the hybrid domain as follows:

(α1) $\alpha = 90$, if $p < p^1$;

(α2) $\alpha = 0$, if $p > p^1$ and $q_a(k+2) > L_{min} q_v(k+2)$;

(α3) $\alpha = \frac{a_l - a_p}{b_p} p$, if $q_a(k+2) = L_{min} q_v(k+2)$, so that the manifold dynamics tracks the fuel dynamics to obtain a mixture with minimum feasible value of A/F ratio.

(α4) $\alpha = -(a_p/b_p)p^1$ when the target set has been reached.

We will now show how to calculate the values of $\Delta(k)$ and $\alpha(t)$.

Consider the cases $p(t_k) < p^1$ (Case 1) and $p(t_k) > p^1$ (Case 2) separately.

- **Case 1:** $p(t_k) < p^1$.

  According to (α1) suppose $\alpha(t) = 90$ for all $t \in [t_k, t_{k+2}]$. Then, the value $p(t_{k+2})$ of the manifold pressure at time t_{k+2} obtained by integration of the pressure dynamics, would be

  $$p(t_{k+2}) = p(t_k) e^{a_p(t_{k+2} - t_k)} - (1 - e^{a_p(t_{k+2} - t_k)}) \frac{90 \cdot b_p}{a_p}\,. \tag{15}$$

  Two cases are possible:

  - **Case 1a:** $p(t_{k+2}) \leq p^1$

    In this case, we can indeed set $\alpha(t) = 90$ for all $t \in [t_k, t_{k+2}]$ and only the value of $\Delta(k)$ needs to be computed. In order to compute the value of $\Delta(k)$ the amount of fuel $q_v(k+2)$ loaded in the cylinder at time t_{k+2} needs to be evaluated. Integration of the fuel dynamics gives:

    $$q_v(k+2) = \left(1 - e^{-\frac{t_{k+2} - t_{k-2}}{\tau}}\right) m_l(t_{k-2}) + e^{-\frac{t_{k+2} - t_k}{\tau}} e^{\frac{t_d}{\tau}} \left(1 - e^{\frac{\Delta}{\tau}}\right) \chi P \tau + P \Delta\,. \tag{16}$$

Hence, according to ($\mathbf{\Delta}1$) and ($\mathbf{\Delta}2$),

$$\Delta(k) = \begin{cases} 0, & \text{if } q_a(k+2) = c_p p(t_{k+2}) < L_{max} q_v^0(k+2); \\ \text{such that } c_p p(t_{k+2}) = L_{max} q_v(k+2), & \text{otherwise;} \end{cases}$$

where[1]

$$q_v^0(k+2) = m_l(t_{k-2})(1 - e^{-\frac{t_{k+2}-t_{k-2}}{\tau}}) \tag{17}$$

is the quantity of fuel loaded at time t_{k+2} if no fuel is injected, i.e. $\Delta(k) = 0$.

- **Case 1b:** $p(t_{k+2}) > p^1$
  In this case, according to ($\alpha 1$) and ($\alpha 4$), α is chosen according to the value of p as:

$$\alpha = \begin{cases} 90, & \text{if } p < p^1 \\ -(a_p/b_p)p^1, & \text{if } p = p^1 \end{cases}$$

  For the injection control[2],

$$\Delta(k) = \begin{cases} 0, & \text{if } q_a(k+2) = c_p p^1 < L_{max} q_v^0(k+2); \\ \text{such that } c_p p^1 = L_{max} q_v(k+2), & \text{otherwise.} \end{cases} \tag{18}$$

- **Case 2:** $p(t_k) > p^1$.
  According to ($\alpha 2$), suppose $\alpha(t) = 0$ for all $t \in [t_k, t_{k+2}]$. Then, the value $p^0(t_{k+2})$ of the manifold pressure at time t_{k+2} would be

$$p^0(t_{k+2}) = p(t_k) e^{a_p(t_{k+2}-t_k)} . \tag{19}$$

  Moreover, suppose $\Delta(k) = 0$ and evaluate the value $q_v^0(k+2)$ of the fuel loaded in the cylinder when $\Delta(k) = 0$ as follows in (17). Then, three cases are possible:

  - **Case 2a:** $p^0(t_{k+2}) \geq p^1$ and $c_p p^0(t_{k+2}) > L_{min} q_v^0(k+2)$.
    Since in this case $p^0(t_{k+2}) \geq p^1$, then we can indeed set $\alpha = 0$ for all $t \in [t_k, t_{k+2}]$ and only the value of $\Delta(k)$ needs to be computed. As shown below, $\Delta(k)$ will be chosen so that $c_p p^0(t_{k+2}) > L_{min} q_v(k+2)$.
    For the injection control, according to ($\mathbf{\Delta}1$) and ($\mathbf{\Delta}2$),

$$\Delta(k) = \begin{cases} 0, & \text{if } c_p p^0(t_{k+2}) < L_{max} q_v^0(k+2); \\ \text{such that } c_p p^0(t_{k+2}) = L_{max} q_v(k+2), & \text{otherwise.} \end{cases}$$

  - **Case 2b:** $p^0(t_{k+2}) < p^1$ and $c_p p^0(t_{k+2}) > L_{min} q_v^0(k+2)$.
    According to ($\alpha 2$) and ($\alpha 4$), α is chosen according to the value of p as:

$$\alpha = \begin{cases} 0, & \text{if } p > p^1 \\ -(a_p/b_p)p^1, & \text{if } p = p^1 \end{cases} . \tag{20}$$

    The injection control is set according to (18).

[1] For both choices of $\Delta(k)$, constraint $c_p p(t_{k+2}) \geq L_{min} q_v(k+2)$ holds. In fact, when $\Delta = 0$, $c_p p(t_{k+2}) > c_p p(t_k) \geq L_{min} q_v(k) > L_{min} q_v^0(k+2)$, and when $\Delta \neq 0$, $c_p p(t_{k+2}) = L_{max} q_v(k+2) > L_{min} q_v(k+2)$.

[2] As in **Case 1a**, constraint $c_p p^1 \geq L_{min} q_v(k+2)$ holds for both choices of $\Delta(k)$.

– **Case 2c:** $c_p p^0(t_{k+2}) \leq L_{min} q_v^0(k+2)$.

This case contains the case where a sliding motion was enforced in the continuous time model to satisfy the A/F constraints. In particular, when the value of $q_v^0(k+2)$ is greater than $c_p p^1/L_{min}$, the throttle control action must be modified in order to load a greater amount of air to fulfill the A/F constraints.

If $q_v^0(k+2) \leq c_p p^1/L_{min}$ then necessarily $p^0(t_{k+2}) \leq p^1$ and this case reduce to the Case 2b and (20), (18) are applied. On the contrary, if $q_v^0(k+2) > c_p p^1/L_{min}$ then $\Delta(k) = 0$ and α must be chosen so that $c_p p(t_{k+2}) = L_{min} q_v^0(k+2)$, that is

$$\alpha(t) = \begin{cases} 0\,, & \text{if } c_p p(t) > L_{min}\left(1 - e^{\frac{t-t_{k+2}}{\tau}}\right) m_l(t_{k-2}); \\ \frac{a_l - a_p}{b_p} p(t)\,, & \text{otherwise.} \end{cases} \tag{21}$$

It is worth noting that the previous hybrid control law cannot be applied if the following four problems are not solved:

Pb. 1 At each dead–center time t_k, the controller needs the value of the time t_{k+2}, corresponding to two dead–centers ahead, to compute the injection time $\Delta(k)$ for the cylinder that enters the exhaust stroke.

Pb. 2 At each dead–center time t_k, the controller has to estimate the value of the mass of liquid fuel $m_l(t_{k-2})$ the cylinder under control had at t_{k-2}.

Pb. 3 When fuel injection is not zero, the controller has to solve an algebraic equation containing the nonlinear term given in (16) to set the value of $\Delta(k)$.

Pb. 4 Since the control law for $\alpha(t)$ is given for two strokes, i.e. for $t \in [t_k, t_{k+2}]$, then it must be shared among two different cylinders for each stroke.

In the design of the hybrid controller, the above concerns are addressed by means of the following arguments:

Sol. 1 Assuming

$$|\omega(t) - \omega(t_k)| \leq \Omega \quad \text{for all } t \in [t_k, t_{k+2}]\,, \ \ \forall t_k\,, \tag{22}$$

the values of $t_{k+2} - t_k$ and $t_{k+2} - t_{k-2}$ are bounded by

$$2\pi/(\omega(t_k) + \Omega) \leq t_{k+2} - t_k \leq 2\pi/(\omega(t_k) - \Omega)\,, \ \ \forall t_k\,, \tag{23}$$

$$4\pi/(\omega(t_k) + 2\Omega) \leq t_{k+2} - t_{k-2} \leq 4\pi/(\omega(t_k) - 2\Omega)\,, \ \ \forall t_k\,. \tag{24}$$

The approximation by defect or by excess will be appropriately used in the design of the hybrid control laws, precisely in equations (15), (16), (17) and (19), in order to ensure convergence to the target set and constraints satisfaction.

Sol. 2 We will assume to know the value of the fuel liquid mass at the beginning of the horizon of control. This is a fair assumption when the system evolves from a steady state condition with injectors having the same characteristics. Indeed, measurements from UEGO sensor can be used to estimate the fuel mass steady state value. Then, for each cylinder, the value of the liquid mass fuel can be obtained by forwards integration of the fuel dynamics.

Sol. 3 Equation (16) can be linearized with respect to Δ by replacing $\tau\left(1 - e^{\frac{\Delta}{\tau}}\right)$ with $-\Delta$ for instance. A conservative linear approximation will be used in the hybrid control law in order to ensure convergence and satisfaction of the constraints.

Sol. 4 At time t_k, the controller determines the value of the throttle control for $t \in [t_k, t_{k+2}]$ and evaluates the value the manifold pressure p will have at time t_{k+2}, on the basis of the current value of manifold pressure $p(t_k)$. To be able to interleave the actions on the throttle control for different cylinders, so that the constraints on the A/F ratio are verified for all cylinders, the previous strategy is modified as follows: at time t_k the controller determines the value of the throttle control in the smaller interval $[t_{k+1}, t_{k+2}]$ on the basis of an estimate of the manifold pressure at time t_{k+1} and of the throttle control set at the time t_{k-1} and acting on the interval $[t_k, t_{k+1}]$. Accordingly, cases 1 and 2 are distinguished on the basis of an estimate of the value $p(t_{k+1})$ and equations (15) and (19) are appropriately modified using bounds:

$$\pi/(\omega(t_k) + \Omega) \leq t_{k+2} - t_{k+1} \leq \pi/(\omega(t_k) - \Omega)\,, \quad \forall t_k\,.$$

The hybrid injection control Δ law is summarized in Figure 3.

The satisfaction of the air-fuel ratio constraints for the hybrid closed–loop system is guaranteed by the following theorem.

Theorem 2 *Given the engine hybrid model $\mathcal{E}$, let $K = \left(e^{\frac{\Delta_{max}}{\tau}} - 1\right) e^{\frac{t_d}{\tau}} \frac{\tau}{\Delta_{max}}$ and $D = e^{\frac{t_d}{\tau}}$. If*

$$\chi K \leq 1 \quad \textit{and} \quad \frac{\chi\,(K L_{max} - D L_{min})}{L_{max} - L_{min}} \leq 1\,, \tag{25}$$

then there exists a value $\Omega > 0$, such that if $\omega(t)$ is bounded as in equation (22), then constraints (5) are satisfied along the trajectory of the closed–loop hybrid system obtained applying the injection feedback control law given in Figure 3 to the engine hybrid model $\mathcal{E}$.

Proof. Consider first the case $\alpha = 0$. By (19), applying approximations (23), $q_a(k+2)$ can be bounded as follows:

$$c_p \underline{p}(k+2) \leq q_a(k+2) \leq c_p \overline{p}(k+2)\,, \tag{26}$$

where

$$\underline{p}(k+2) \;=\; e^{\frac{\pi a_p}{\omega(t_k)+\Omega}} p(t_{k+1}) \leq p(t_{k+2})\,, \tag{27}$$

$$\overline{p}(k+2) \;=\; e^{\frac{\pi a_p}{\omega(t_k)-\Omega}} p(t_{k+1}) \geq p(t_{k+2})\,. \tag{28}$$

Further, by (16), (23) and (24), $q_v(k+2)$ can be bounded by

$$\underline{q}_v(k+2) \leq q_v(k+2) \leq \overline{q}_v(k+2)\,,$$

with

$$\underline{q}_v(k+2) \leq (1 - e^{-\frac{4\pi/\tau}{\omega(t_k)+2\Omega}}) m_l(t_{k-2}) + e^{-\frac{2\pi/\tau}{\omega(t_k)+\Omega}} e^{\frac{t_d}{\tau}} \left(1 - e^{\frac{\Delta}{\tau}}\right) \chi P \tau + P\Delta\,, \tag{29}$$

$$\overline{q}_v(k+2) \geq (1 - e^{-\frac{4\pi/\tau}{\omega(t_k)-2\Omega}}) m_l(t_{k-2}) + e^{-\frac{2\pi/\tau}{\omega(t_k)-\Omega}} e^{\frac{t_d}{\tau}} \left(1 - e^{\frac{\Delta}{\tau}}\right) \chi P \tau + P\Delta\,, \tag{30}$$

where[3] $K = \left(e^{\frac{\Delta_{max}}{\tau}} - 1\right) e^{\frac{t_d}{\tau}} \frac{\tau}{\Delta_{max}}$ and $D = e^{\frac{t_d}{\tau}}$, with $K \geq D$.

Hence, constraints (5) are guaranteed to be satisfied if there exists a value Δ for the injection control such that

$$\begin{aligned} L_{min}\overline{q}_v(k+2) &\leq c_p\underline{p}(k+2)\,, \qquad (31)\\ L_{max}\underline{q}_v(k+2) &\geq c_p\overline{p}(k+2)\,, \qquad (32)\end{aligned}$$

with upper and lower bounds given by (27), (28), (29) and (30).

Indeed, by construction, for this value of Δ we have

$$\begin{aligned} L_{min}q_v(k+2) \leq L_{min}\overline{q}_v(k+2) \leq c_p\underline{p}(k+2) \leq c_p p(t_{k+2}) = q_a(k+2)\,,\\ L_{max}q_v(k+2) \geq L_{max}\underline{q}_v(k+2) \geq c_p\overline{p}(k+2) \geq c_p p(t_{k+2}) = q_a(k+2)\,.\end{aligned}$$

To express the condition under which a Δ satisfying both (31) and (32) exists, we select Δ so that (32) is verified with the equality sign, that is, by (28) and (29),

$$\Delta(k) = \frac{c_p e^{\frac{\pi a_p}{\omega(t_k)-\Omega}} p(t_{k+1}) - L_{max}\left(1 - e^{-\frac{4\pi/\tau}{\omega(t_k)+2\Omega}}\right) m_l(t_{k-2})}{L_{max}\left(1 - \chi K e^{-\frac{2\pi/\tau}{\omega(t_k)+\Omega}}\right) P}\,, \qquad (33)$$

and plug this value into (31). In order to obtain the sufficient condition (25), let us compute the limit of the inequality (31) as $\Omega \longrightarrow 0$. When $\Omega \longrightarrow 0$, (31) is satisfied iff

$$\mathcal{F}(\omega(t_k))\, m_l(t_{k-2}) \leq \mathcal{G}(\omega(t_k))\, e^{\frac{\pi a_p}{\omega(t_k)}} c_p p(t_{k+1})\,, \qquad (34)$$

where

$$\mathcal{F}(\omega(t_k)) = \frac{-\chi(K-D)\left(1 - e^{-\frac{4\pi/\tau}{\omega(t_k)}}\right) e^{-\frac{2\pi/\tau}{\omega(t_k)}}}{\left(1 - \chi D e^{-\frac{2\pi/\tau}{\omega(t_k)}}\right)\left(1 - \chi K e^{-\frac{2\pi/\tau}{\omega(t_k)}}\right)}$$

and

$$\mathcal{G}(\omega(t_k)) = \frac{L_{max}\left(1 - \chi K e^{-\frac{2\pi/\tau}{\omega(t_k)}}\right) - L_{min}\left(1 - \chi D e^{-\frac{2\pi/\tau}{\omega(t_k)}}\right)}{L_{min}\left(1 - \chi D e^{-\frac{2\pi/\tau}{\omega(t_k)}}\right) L_{max}\left(1 - \chi K e^{-\frac{2\pi/\tau}{\omega(t_k)}}\right)}\,.$$

If, according to (25), $\chi K \leq 1$, then $\chi D \leq 1$. Further, since $\omega(t_k) > 0$, then $e^{-\frac{2\pi/\tau}{\omega(t_k)}} < 1$ and $e^{-\frac{4\pi/\tau}{\omega(t_k)}} < 1$. Hence, being $K > D$ and $m_l(t_{k-2}) > 0$, the term on the left hand side is negative. Furthermore, note that $e^{\frac{\pi a_p}{\omega(t_k)}} > 0$, $c_p > 0$ and $p(t_{k+1}) > 0$. Hence if, as in (25), $\frac{\chi(KL_{max} - DL_{min})}{L_{max} - L_{min}} \leq 1$, then the term on the right hand side is not negative and (34) is verified. Then, being (34) verified under conditions (25), by continuity of (31) with respect to Ω, there exists a small enough Ω satisfying it.

[3] In fact, $\left(1 - e^{\frac{\Delta_{max}}{\tau}}\right) \frac{\tau}{\Delta_{max}}\Delta \leq \tau\left(1 - e^{\frac{\Delta}{\tau}}\right) \leq -\Delta, \quad \forall\Delta \in [0, \Delta_{max}]$. Since $\Delta_{max} \ll \tau$, then this approximations are both close to the real value.

The same argument applies when considering the other cases. In the case where $\alpha = 90$, the upper and lower bounds in (26) are as follows

$$\underline{p}(k+2) = e^{\frac{\pi a_p}{\omega(t_k)+\Omega}} p(t_{k+1}) - (1 - e^{\frac{\pi a_p}{\omega(t_k)+\Omega}}) \frac{90 \cdot b_p}{a_p} \leq p(t_{k+2}) \,, \tag{35}$$

$$\overline{p}(k+2) = e^{\frac{\pi a_p}{\omega(t_k)-\Omega}} p(t_{k+1}) - (1 - e^{\frac{\pi a_p}{\omega(t_k)-\Omega}}) \frac{90 \cdot b_p}{a_p} \geq p(t_{k+2}) \,. \tag{36}$$

By using (35) and (36), in place of (27) and (28), we get

$$\Delta(k) = \frac{c_p e^{\frac{\pi a_p}{\omega(t_k)-\Omega}} p(t_{k+1}) - c_p(1 - e^{\frac{\pi a_p}{\omega(t_k)-\Omega}}) \frac{90 \cdot b_p}{a_p} - L_{max}\left(1 - e^{-\frac{4\pi/\tau}{\omega(t_k)+2\Omega}}) m_l(t_{k-2})\right)}{L_{max}\left(1 - \chi K e^{-\frac{2\pi/\tau}{\omega(t_k)+\Omega}}\right) P} \,. \tag{37}$$

Then (31), when $\Omega \longrightarrow 0$, reduces to

$$\mathcal{F}(\omega(t_k))\, m_l(t_{k-2}) \leq \mathcal{G}(\omega(t_k))\, e^{\frac{\pi a_p}{\omega(t_k)}} c_p p(t_{k+1}) - \left(1 - e^{\frac{\pi a_p}{\omega(t_k)}}\right) \frac{90 \cdot b_p c_p}{a_p} \,. \tag{38}$$

As in the previous case, the term on the left hand side of (38) is negative. Moreover, since $0 < e^{\frac{\pi a_p}{\omega(t_k)}} < 1$ and $90 \cdot b_p / a_p < 0$, then the term on the right hand side is not negative and the inequality is verified. Hence, there exists Ω small enough such that condition (31) is satisfied for any feasible value of $p(t_{k+1})$ and $m_l(t_{k-2})$, so that the injection controls (33) and (37), applied when $\alpha = 0$ and $\alpha = 90$ respectively, approximate the control ($\mathbf{\Delta}2$), i.e. $q_a(k+2) \approx L_{max} q_v(k+2)$, guaranteeing that the A/F ratio constraints (5) are met for the hybrid model.

Consider now the case where the manifold dynamics follows the fuel dynamics, i.e. controls ($\mathbf{\Delta}1$) and ($\alpha 3$) are applied. Since in this condition the fuel injection control is $\Delta = 0$, then the liquid fuel dynamics evolves in free motion and the continuous throttle control (21) guarantees that the constraint $q_a(k+2) = L_{min} q_v(k+2)$ is followed precisely, no matter of the approximation on the time t_{k+2}.

Finally, when the hybrid system has converged to the target and the manifold control $\alpha = \frac{a_p}{b_p} p^1$ is applied, the injection control is simply

$$\Delta(k) = \frac{p^1 - L_{max}\left(1 - e^{-\frac{4\pi/\tau}{\omega(t_k)+2\Omega}}) m_l(t_{k-2})\right)}{L_{max}\left(1 - \chi K e^{-\frac{2\pi/\tau}{\omega(t_k)+\Omega}}\right) P} \,. \tag{39}$$

Then (31), when $\Omega \longrightarrow 0$, reduces to

$$\mathcal{F}(\omega(t_k))\, m_l(t_{k-2}) \leq \mathcal{G}(\omega(t_k))\, c_p p^1 \,.$$

Since the right hand side is not negative, then there exists Ω small enough such that condition (31) is satisfied for any feasible value of $p(t_{k+1})$ and $m_l(t_{k-2})$, so that the injection controls (33), (37), and (39), applied when $\alpha = 0$, $\alpha = 90$, and $\alpha = -(a_p/b_p)p^1$ respectively, guarantee that the A/F ratio constraints (5) are met for the hybrid model. Q.E.D.

Conditions (25) of Theorem 2 are usually verified by models of commercial cars. If we restrict the range of variability of the model by examining particular cases of commercial cars, a less restrictive value of Ω can be given. For example, if we use the parameters as in Table 1 corresponding to the model of a commercial car, we can claim:

Theorem 3 *If at the initial time the engine hybrid model $\mathcal{E}$ with parameters as in Table 1 is at the steady state corresponding to a given initial torque u^0 with stoichiometric mixture, then the injection feedback control law given in Figure 3 guarantees that constraints (5) are satisfied along the trajectory of the closed–loop hybrid system for every desired torque u^1, if $\omega(t) \geq 1200 rpm$ and*

$$\Omega \quad = \quad 17rpm, \quad \text{when } L_{min} = 0.97L_{stc} \text{ and } L_{max} = 1.03L_{stc},$$

that is for all the operating conditions of the engine.

Proof. For the sake of brevity, we report here only the proof for the case $\alpha = 0$. The result is proved by bounding in a conservative way the evolution of the sequences $m_l(t_{k-2})$ and $c_p p(t_{k+1})$, when starting from an initial steady state, so that (31) is guaranteed to be satisfied.

When the engine is at the steady state corresponding to a given fuel injection time Δ, if the mixture is at stoichiometry, for all $k = 4i + 1 \leq 1$, we have

$$\begin{aligned} m_l(t_{k-2}) &= m_l^{\Delta} = \frac{e^{-\frac{2\pi/\tau}{\omega(t_k)}} e^{\frac{t_d}{\tau}} \left(e^{\frac{\Delta}{\tau}} - 1\right) \chi P \tau}{1 - e^{-\frac{4\pi/\tau}{\omega(t_k)}}}, \\ c_p p(t_{k+1}) &= c_p p^{\Delta} = e^{-\frac{\pi a_p}{\omega(t_k)}} L_{stc} P \Delta . \end{aligned}$$

When the control $\alpha = 0$ is applied, since $(e^{\frac{\Delta}{\tau}} - 1)\tau$ increases more that Δ, when Δ increases, then the worst case with respect to the inequality (31) is that of starting from the steady state corresponding to $\Delta = \Delta_{max}$. Indeed, in this case, we have that

- at the starting steady state point $m_l(t_{k-2})$ is the largest possible value (namely $m_l^{\Delta_{max}}$) with respect to the correspoding value of $c_p p(t_{k+1})$ (namely $c_p p^{\Delta_{max}}$); and
- in the following evolution the fuel film evaporation is the longest one due to the high quantity of fuel puddle mass, while the manifold pressure reaches soon low values under the action of $\alpha = 0$.

The value of the crankshaft speed $\omega(t_k)$ depends on the enganged gear and the car load torques.

Note that, by (22), it follows that

$$\begin{aligned} 4\pi/(\omega(t_k) + 4\Omega) \leq t_{k-2} - t_{k-6} \leq 4\pi/(\omega(t_k) - 4\Omega) , \\ 2\pi/(\omega(t_k) + 3\Omega) \leq t_{k-2} - t_{k-4} \leq 2\pi/(\omega(t_k) - 3\Omega) , \\ 4\pi/(\omega(t_k) + 3\Omega) \leq t_{k+1} - t_{k-3} \leq 4\pi/(\omega(t_k) - 3\Omega) . \end{aligned}$$

a_α	$-.2805$	b_α	$.7126$	τ	$.20$	Δ_{max}	$5\,10^{-3}$	P	$G_f\frac{\omega(t_k)}{\pi}$
a_p	-14.61	b_p	$5.143\,10^6$	t_d	$5\,10^{-4}$	χ	$.5$	G_f	$1.93\,10^{-3}$

Table 1: Hybrid engine model $\mathcal{E}$ parameters.

Hence, in the closed–loop hybrid system, the evolutions of $m_l(t_{k-2})$ and $c_pp(t_{k+1})$, for $k = 4i+1 > 1$, are bounded as follows:

$$\begin{aligned} m_l(t_{k-2}) &= e^{-\frac{t_{k-2}-t_{k-6}}{\tau}} m_l(t_{k-6}) + \left(e^{\frac{\Delta(k-4)}{\tau}} - 1\right) e^{-\frac{t_{k-2}-t_{k-4}}{\tau}} D\chi P\tau \\ &\leq e^{-\frac{4\pi/\tau}{\omega(t_k)+4\Omega}} m_l(t_{k-6}) + \left(e^{\frac{\Delta(k-4)}{\tau}} - 1\right) e^{-\frac{2\pi/\tau}{\omega(t_k)+3\Omega}} D\chi P\tau\,, \end{aligned} \tag{40}$$

$$c_pp(t_{k+1}) = e^{a_p(t_{k+1}-t_{k-3})} c_pp(t_{k-3}) \geq e^{\frac{4\pi a_p}{\omega(t_k)-3\Omega}} c_pp(t_{k-3})\,, \tag{41}$$

where $\Delta(k-4)$ is computed according to (33). Expresions (40) and (41) are iteratively computed to provide upper and lower bounds, respectively, for $m_l(t_{k-2})$ and $c_pp(t_{k+1})$ in (31), till a negative value of Δ is given by (33) which corresponds to the end of control action $\alpha = 0$.

With the parameters given in Table 1, the maximum value of Ω for which constraint (31) is guaranteed is

$$\Omega = 17\text{rpm}, \text{ if } L_{min} = 0.97L_{stc} \text{ and } L_{max} = 1.03L_{stc}\,.$$

Q.E.D.

5 Control with throttle dynamics

In this section, we re-introduce the throttle actuation dynamics. As in the previous case, we progress from the continuous approximation to the full hybrid model. The difference with the previous case is that, in this case we are able to prove the optimality property of the control law derived for the continuous approximation, but the shear complexity of the hybrid problem makes the proof of the properties of the hybrid control law derived from the continuous law extremely complicated. For this reason, we do not carry through all the (tedious) derivations and we simply show the quality of the control on an example of a power train of a commercial car.

5.1 Continuous Approximation

The hybrid nature of the intake process is abstracted away by using the average continuous–time model introduced in Section 3 for fuel flow and equations (1)–(2) for air flow. As in Section 3, the flow of air $f_a(t)$ entering the cylinders is expressed as $f_a(t) = c_ap(t)$.

To solve the continuous optimal problem, we follow a two-step process: in the first step, we find the minimum–time control for the air dynamics (1)–(2) alone; in the second step, we introduce the fuel dynamics and appropriately modify the optimal control law found in the first step to solve the continuous optimal problem.

The target set corresponding to the desired torque u^1 becomes now

$$\widetilde{\mathcal{T}}(u^1) = \left\{ (\overline{m}_l, \alpha, p) |\ \alpha = \alpha^1 = -\frac{a_p}{b_p} \frac{14.64}{c_p G} u^1, p = p^1 = \frac{14.64}{c_p G} u^1 \right\}. \tag{42}$$

Since the input v is constrained to belong to $[-V, +V]$ while α must remain within the interval $[0, 90]$, then Problem 1 reduces to the following one:

Problem 3 *Consider the engine continuous–time model described by equations (1), (2) and (6). Let u^0 and u^1 be the initial value and the desired value of the torque, respectively. Assume that, at the initial time $t = 0$, the state $(\overline{m}_l^0, \alpha^0, p^0)$ belongs to $\widetilde{\mathcal{T}}(u^0)$. Find $\hat{v}(t) : \mathbb{R}_0^+ \to [-V, +V]$ and $\hat{\Delta}(t) : \mathbb{R}_0^+ \to [0, \Delta_{max}]$ such that*

- *the initial state $(\overline{m}_l^0, \alpha^0, p^0)$ is steered to $\widetilde{\mathcal{T}}(u^1)$ at some unspecified time $t^\star$;*
- *for all $t \geq 0$, constraints (4) and (7) are satisfied;*
- *the time $t^\star$ is minimized.*

To solve this problem, we first compute the minimum–time control to the target point $\{\alpha = \alpha^1, p = p^1\}$ for the intake manifold dynamics (1)–(2) alone in the subspace (α, p), and then we study the optimal solution when the fuel dynamics (6) and the constraints (7) are considered.

Figure 4 shows the synthesis of minimum–time trajectories to the target point $\{\alpha = \alpha^1, p = p^1\}$ in the subspace (α, p). The minimum–time control law is the following state feedback:

$$v = \begin{cases} +V & \text{if } (\alpha, p) \text{ is below } \gamma \text{ or lays on } \gamma_+ \\ -V & \text{if } (\alpha, p) \text{ is above } \gamma \text{ or lays on } \gamma_- \\ 0 & \text{if } \alpha = 0 \text{ and } (\alpha, p) \text{ is over } \gamma \end{cases}$$

where $\gamma = \gamma_- \cup \gamma_+$ is the switching curve and γ_- and γ_+ are the trajectories obtained by backwards integration of dynamics (1)–(2) from the target point (α^1, p^1) with $v = -V$ and $v = +V$, respectively.

Initial conditions lying below γ are first steered by the control $v = +V$ to γ_- and then to the target point along γ_- by the control $v = -V$. On the other hand, initial conditions above γ are first steered by the control $v = -V$ to either γ_+ or to the set $\alpha = 0$. If the set $\alpha = 0$ is reached, then the singular control $v = 0$ is applied until γ_+ is reached. Then, the state is steered to the target point along γ_+ by the control $v = +V$.

Consider now the dynamics (6) together with the constraints (7).

First of all, note that not all the initial conditions in the feasible set defined by (9) can be driven to the target set satisfying constraints (7). Indeed, consider for example states $(\overline{m}_l, \alpha, p)$ lying on the boundary $L_1 p + L_m \overline{m}_l = 0$ of the feasible set and such that

$$L_1 a_p p + L_1 b_p \alpha + L_m a_l \overline{m}_l < 0.$$

Since $L_m b_l < 0$ and $\Delta \geq 0$, then

$$L_1 \dot{p} + L_m \dot{\overline{m}}_l = L_1(a_p p + b_p \alpha) + L_m(a_l \overline{m}_l + b_l \Delta) \leq L_1(a_p p + b_p \alpha) + L_m a_l \overline{m}_l < 0\,.$$

Then, the evolution through these feasible states will unavoidably violate constraints (7) no matter how the control actions for v and Δ are chosen.

Hence, the boundary of the set of states that can be driven to the target set by means of trajectories satisfying constraints (7) is given by the surface Φ_{inf} obtained by backwards integration of dynamics (1), (2) and (6) from the line

$$\begin{cases} L_1 p + L_m \overline{m}_l = 0 \\ L_1 a_p p + L_1 b_p \alpha + L_m a_l \overline{m}_l = 0 \end{cases} \tag{43}$$

with controls $v = +V$ and $\Delta = \max\{0, L_2 p + L_m \overline{m}_l\}$. See Figure 5. The same argument applies when considering the upper boundary $L_2 p + L_m \overline{m}_l = \Delta_{max}$ of the feasible set. In this case the boundary is given by the surface Φ_{sup} obtained by backwards integration of dynamics (1), (2) and (6) from the line

$$\begin{cases} L_2 p + L_m \overline{m}_l = \Delta_{max} \\ L_2 a_p p + L_2 b_p \alpha + L_m a_l \overline{m}_l = -L_m b_l \Delta_{max} \end{cases}$$

with controls $v = -V$ and $\Delta = \max\{0, L_2 p + L_m \overline{m}_l\}$.

From now on, we will consider only initial conditions that are feasible and controllable to the target set while satisfying constraints (7), i.e., initial conditions satisfying inequalities (9) and between the surfaces Φ_{inf} and Φ_{sup}. For the sake of brevity, we will denote such conditions as *feasible and controllable*. Moreover, for the sake of simplicity, we will assume that the surface Φ_{sup} is never reached.

The following theorem holds:

Theorem 4 *Define* $\Gamma = \Gamma_- \cup \Gamma_+$, *with*

$$\Gamma_- = \{(\overline{m}_l, \alpha, p) |\ (\alpha, p) \in \gamma_-\}, \qquad \Gamma_+ = \{(\overline{m}_l, \alpha, p) |\ (\alpha, p) \in \gamma_+\}.$$

If the initial state $(\overline{m}_l^0, \alpha^0, p^0)$ *is feasible and controllable, then the optimal control* $\hat{v}(t) : \mathbb{R}_0^+ \to [-V, +V]$ *and* $\hat{\Delta}(t) : \mathbb{R}_0^+ \to [0, \Delta_{max}]$ *solving Problem 3 is:*

$$\hat{v} = \begin{cases} -V & \text{if } (\overline{m}_l, \alpha, p) \text{ lays on } \Gamma_- \text{ or it is above } \Gamma \text{ and either belongs} \\ & \text{to the interior of the set of feasible and controllable states} \\ & \text{or } L_1 p + L_m \overline{m}_l = 0 \text{ and } (\overline{m}_l, \alpha, p) \notin \Phi_{inf} \\ 0 & \text{if } \alpha = 0,\ (\overline{m}_l, \alpha, p) \text{ is above } \Gamma \text{ and } (\overline{m}_l, \alpha, p) \notin \Phi_{inf} \\ +V & \text{if either } (\overline{m}_l, \alpha, p) \text{ is above } \Gamma,\ (\overline{m}_l, \alpha, p) \in \Phi_{inf} \text{ and } L_1 p + \\ & L_m \overline{m}_l > 0 \text{ or } (\overline{m}_l, \alpha, p) \text{ is below } \Gamma \text{ or lays on } \Gamma_+ \\ \frac{a_l - a_p}{b_p} \frac{a_l - a_\alpha}{b_\alpha} p & \text{if } (\overline{m}_l, \alpha, p) \text{ is above } \Gamma \text{ and belongs to the line (43)} \\ \frac{-a_\alpha}{b_\alpha} \alpha^1 & \text{if } (\overline{m}_l, \alpha, p) \text{ lays on } \widetilde{\mathcal{T}}(u^1) \end{cases}$$

$$\hat{\Delta} = \max\{0, L_2 p + L_m \overline{m}_l\}.$$

5.2 Hybrid Problem

Along the same lines of Section 4, the continuous optimal control is mapped into the hybrid domain by first computing the values of $\Delta(k)$ and $v(t)$ assuming knowledge of the exact value of time t_{k+2}. Then, the hybrid control is obtained by appropriately approximating by defect or by excess t_{k+2} as in (23).

To map the continuous control law into values of $\Delta(k)$ and $v(t)$, we have to evaluate the values of α, p and m_l at time t_{k+2}. According to the estimated values of those quantities, several different cases have to be analyzed. Consider, for example, the case corresponding to $(\alpha(t_k), p(t_k))$ below γ (Case 1). This case has to be split in two subcases:

Case 1a $(\alpha(t_{k+2}), p(t_{k+2}))$ below γ;

Case 1b $(\alpha(t_{k+2}), p(t_{k+2}))$ above γ;

In the first case the control $v(t)$ is set to $+V$ for all $t \in [t_k, t_{k+2}]$ and $\Delta(k)$ is chosen on the basis of the computation of the amount of air $q_a(k+2)$ and fuel $q_v(k+2)$ loaded in the cylinder at time t_{k+2}. In the second case $v(t)$ is set to $+V$ until γ is reached and then is set to $-V$. This corresponds to $(\alpha(t), p(t))$ moving on γ_- and two different sub-subcases are possible:

Case 1b.1 $\alpha(t_{k+2}) > \alpha^1$;

Case 1b.2 $\alpha(t_{k+2}) \leq \alpha^1$;

In the first case $v(t)$ has not to be changed, while in the second case one has to set $v(t) = -a_\alpha \alpha^1 / b_\alpha$ when the point (α^1, p^1) is reached. As in Section 4, $\Delta(k)$ is chosen on the basis of the computation of the amount of air $q_a(k+2)$ and fuel $q_v(k+2)$ loaded in the cylinder at time t_{k+2}.

When considering the case corresponding to $(\alpha(t_k), p(t_k))$ above γ (Case 2), a number of cases and subcases have to be considered. These cases correspond to the different possible position of $(\alpha(t_{k+2}), p(t_{k+2}), m_l(t_{k+2}))$ with respect to Γ, Φ_{inf}, and the planes $L_1 p + L_m m_l = 0$ and $\alpha = 0$. Moreover, each case may need to be split in several subcases so that the complete analysis is very complex to expound. In all these cases, the value of $\Delta(k)$ is chosen on the basis of the computation of the amount of air $q_a(k+2)$ and fuel $q_v(k+2)$ loaded in the cylinder at time t_{k+2}.

When the values of $v(t)$ and $\Delta(k)$ have been computed, then the hybrid control law is obtained by appropriately approximate time t_{k+2} by defect or by excess using (23) as for the injection feedback control given in Figure 3 .

The analysis of constraints satisfaction is, in this case, very complex and tedious. The behavior of the resulting hybrid control has been tested by running simulations of the hybrid closed–loop system. We now report some of these results.

Figures 6 show the results of the proposed approach when the engine is requested to change the produced torque from the initial constant value $u^0 = 35$ Nm to the final constant value $u^1 = 10$ Nm, with initial crankshaft velocity 4000 rpm. The air–to–fuel ratio is requested to remain within a 3% band centered around the stoichiometric value.

The control starts at $t_0 = 0.052$ seconds from the steady state corresponding to u^0. The throttle valve is forced to close as fast as possible under the initial control $v(t) = -V$, while fuel injection is controlled so that A/F is maintained on the maximum feasible value. When the valve is about to close, at time $t = 0.061$ seconds, $v(t)$ is set to 0. At time $t = 0.105$ seconds, the switching surface Γ^+ is approached and the control $v(t)$ is set to V. Then, at time $t = \bar{t} = 0.108$ seconds, the throttle position and the manifold pressure are close to the target point (α^1, p^1) and the input v is set to the equilibrium value $-\frac{a_\alpha}{b_\alpha}\alpha^1$. The corresponding value of torque is generated during the expansion stroke starting at time $t = 0.12$ seconds. Note that no significant undershoot is exhibited with respect to the reference value u^1. Starting from the first dead–center after time $\bar{t}$, that is at time $\hat{t} = 0.117$ seconds, fuel injection is regulated so to obtain a stoichiometric air–fuel ratio. Note that, the evolution of the fuel injection signal $\Delta(k)$ - and consequently that of $A/F(k)$ - exhibits oscillations of 4–sample period for times greater than $\hat{t}$. This behavior is due to the fact that the injection signal Δ represents the four injection durations $\Delta_1, \ldots, \Delta_4$ related to the four independent fuel dynamics, which have different fuel puddle. Moreover, dead-center times estimation errors due to the crankshaft speed evolution, results in an additional noise on $\Delta(k)$ that tends to zero as the crankshaft speed approaches the equilibrium value.

6 Conclusions

The problem of delivering as quickly as possible a requested torque produced by a spark ignition engine equipped with a multi-point port injection manifold and with electronic–throttle control has been addressed. The optimization problem, subject to the constraint that the air–fuel ratio stays within a pre–assigned range around the stoichiometric ratio, has been solved using hybrid systems modeling and control approaches. The solution to the control problem is obtained by a two-step process that consists in first introducing and solving an auxiliary optimal control problem in the continuous time domain, and then in mapping the optimal control law back into the hybrid domain. To show the proposed design approach without excessive complexity, we neglected the nonlinearities and the dependence of the pressure dynamics and of the expression of the generated torque on engine speed in the plant model of Section (2). To fully leverage the techniques presented in this paper, the model must include these aspects. We plan to address these issues in a forthcoming paper.

7 Acknowledgments

This research has been supported in part by PARADES, a European Economic Interest Group formed by Cadence Design Systems, Magneti Marelli and ST-Microelectronics, CNR, the MADDESSII Special Project of CNR. We wish to thank Dr. Carlo Rossi, Dr. Giovanni Gaviani and their teams at Magneti Marelli for introducing the problem and discussing its solution with us, and Guido Maria Miconi for the simulation results. We wish also to thank the anonymous reviewers of the paper for their insightful comments that have contributed to improve the clarity and the accuracy of the paper.

References

[1] C. F. Aquino, *Transient A/F characteristics of the 5 liter central fuel injection engine*, Tech. Rep. No. 810494, SAE, 1981.

[2] A. Balluchi, M. D. Benedetto, C. Pinello, C. Rossi, and A. Sangiovanni-Vincentelli, *Hybrid control in automotive applications: the cut-off control*, Automatica, 35 (1999), pp. 519–535.

[3] A. Balluchi, A. Bicchi, G. Padroni, C. Rossi, and A. L. Sangiovanni-Vincentelli, *Hybrid optimization problems in automotive applications*, in Proc. IFAC International Workshop on Motion Control, Grenoble, France, September 1998, pp. 273–278.

[4] Y. Chin and F. Coats, *Engine dynamics: time–based versus crank–angle based*, Tech. Rep. No. 860412, SAE, 1996.

[5] E. Hendricks and T. Vesterholm, *The analysis of mean value SI engine models*, Tech. Rep. No. 920682, SAE, 1992.

[6] E. Hendricks, T. Vesterholm, P. Kaidantzis, P. Rasmussen, and M. Jensen, *Nonlinear transient fuel film compensation*, Tech. Rep. No. 930767, SAE, 1993.

[7] U. Lenz and D. Schröder, *Air-fuel ratio control for direct injecting combustion engines using neural networks*, Tech. Rep. No. 981060, SAE, 1998.

[8] F. Maroteaux and L. Le Moyne, *Modeling of fuel deposition rate in port injected spark ignition engine*, Tech. Rep. No. 952484, SAE, 1995.

[9] P. Morall, *Adaptive compensation of fuel dynamics in an SI engine using a switching EGO sensor*, in Proc. CDC95, New Orleans, LA, 1995, pp. 661–666.

[10] C. Vigild, K. Andersen, E. Hendricks, and M. Struwe, *Towards robust H_∞ control of an SI engine's air/fuel ratio*, Tech. Rep. No. 1999-01-0854, SAE, 1999.

BEGIN

$\overline{q}_v^0(k+2) = (1 - e^{-\frac{4\pi/\tau}{\omega(t_k)-2\Omega}})m_l(k-2)$

$\underline{q}_v^0(k+2) = (1 - e^{-\frac{4\pi/\tau}{\omega(t_k)+2\Omega}})m_l(k-2)$

IF $\tilde{p}(k+1) < p^1$ THEN

$\tilde{p}(k+2) = e^{\frac{\pi a_p}{\omega(t_k)}}\tilde{p}(k+1) - (1 - e^{\frac{\pi a_p}{\omega(t_k)}})\frac{90 \cdot b_p}{a_p}$

IF $\tilde{p}(k+2) \leq p^1$ THEN

$\overline{p}(k+2) = e^{\frac{\pi a_p}{\omega(t_k)-\Omega}}\tilde{p}(k+1) - (1 - e^{a_p\frac{\pi}{\omega(t_k)-\Omega}})\frac{90 \cdot b_p}{a_p}$

IF $c_p\overline{p}(k+2) < L_{max}\underline{q}_v^0(k+2)$ THEN

$\Delta(k) = 0$

ELSE $\Delta(k) = \frac{c_p\overline{p}(k+2) - L_{max}\underline{q}_v^0(k+2)}{\left(1-\chi K e^{-\frac{2\pi/\tau}{\omega(t_k)+\Omega}}\right)PL_{max}}$

ELSEIF $\tilde{p}(k+2) > p^1$ THEN

IF $c_p p^1 < L_{max}\underline{q}_v^0(k+2)$ THEN

$\Delta(k) = 0$

ELSE $\Delta(k) = \frac{c_p p^1 - L_{max}\underline{q}_v^0(k+2)}{\left(1-\chi K e^{-\frac{2\pi/\tau}{\omega(t_k)+\Omega}}\right)PL_{max}}$

ELSEIF $\tilde{p}(k+1) > p^1$ THEN

$\tilde{p}(k+2) = e^{\frac{\pi a_p}{\omega(t_k)}}\tilde{p}(k+1)$

$\underline{p}(k+2) = e^{\frac{\pi a_p}{\omega(t_k)-\Omega}}\tilde{p}(k+1)$

IF $\tilde{p}(k+2) \geq p^1$ AND $c_p\underline{p}(k+2) > L_{min}\overline{q}_v^0(k+2)$ THEN

$\overline{p}(k+2) = e^{\frac{\pi a_p}{\omega(t_k)+\Omega}}\tilde{p}(k+1)$

IF $c_p\overline{p}(k+2) < L_{max}\underline{q}_v^0(k+2)$ THEN

$\Delta(k) = 0$

ELSE $\Delta(k) = \frac{c_p\overline{p}(k+2) - L_{max}\underline{q}_v^0(k+2)}{\left(1-\chi K e^{-\frac{2\pi/\tau}{\omega(t_k)+\Omega}}\right)PL_{max}}$

ELSEIF $\tilde{p}(k+2) < p^1$ AND $c_p p^1 > L_{min}\overline{q}_v^0(k+2)$ THEN

IF $c_p p^1 < L_{max}\underline{q}_v^0(k+2)$ THEN

$\Delta(k) = 0$

ELSE $\Delta(k) = \frac{c_p p^1 - L_{max}\underline{q}_v^0(k+2)}{\left(1-\chi K e^{-\frac{2\pi/\tau}{\omega(t_k)+\Omega}}\right)PL_{max}}$

ELSEIF $c_p\underline{p}(k+2) \leq L_{min}\overline{q}_v^0(k+2)$ AND $c_p p^1 \leq L_{min}\overline{q}_v^0(k+2)$ THEN

$\Delta(k) = 0$

END

Figure 3: Hybrid injection control.

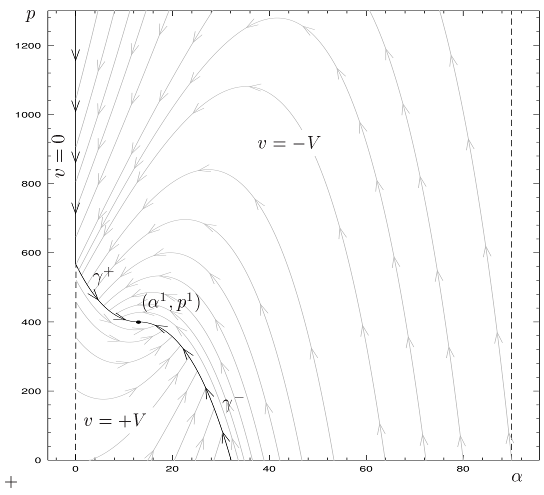

Figure 4: Minimum–time trajectories for throttle dynamics.

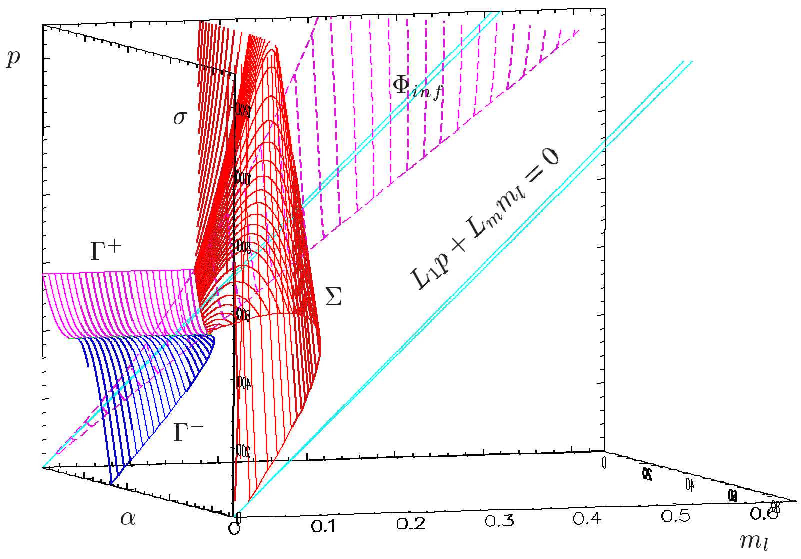

Figure 5: Minimum–time trajectories with throttle dynamics.

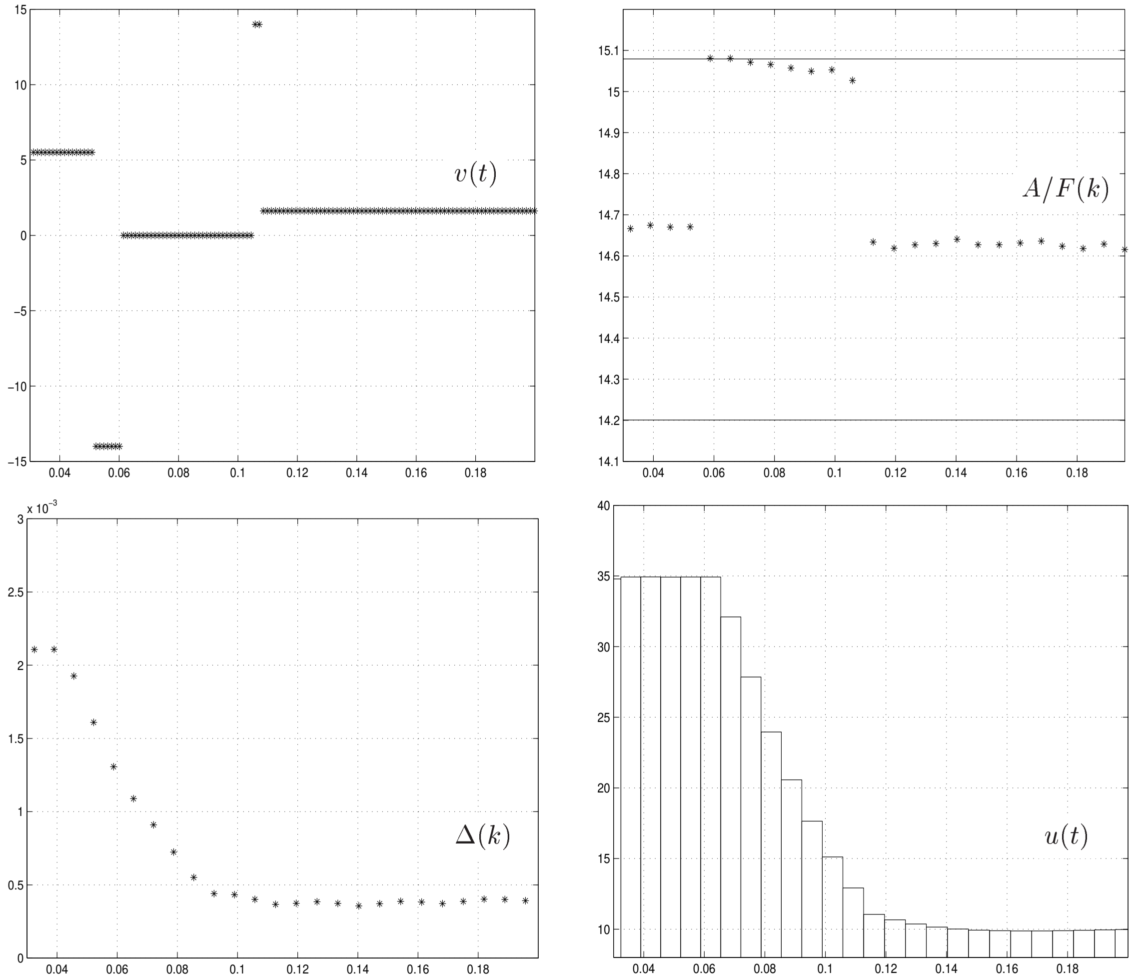

Figure 6: Simulation results: DC motor voltage v and injection times Δ (on the left); air–fuel ratio A/F (at the end of the intake stroke) and generated torque u (on the right).